JACS
JOURNAL OF THE AMERICAN CHEMICAL SOCIETY
Article
pubs.acs.org/JACS

Diphosphine-Stabilized Small Gold Nanoclusters: From Crystal Structure Determination to Ligation-Driven Symmetry Breaking and Anion Exchange Properties

Liao-Yuan Yao and Vivian Wing-Wah Yam*

Institute of Molecular Functional Materials (Areas of Excellence Scheme, University Grants Committee (Hong Kong)) and Department of Chemistry, The University of Hong Kong, Pokfulam Road, Hong Kong 999077, P. R. China

Supporting Information

ABSTRACT: A new class of small gold nanoclusters with molecular characteristics has been constructed using 1,1′-bis(diphenylphosphino)ferrocene (dppf) as the stabilizing ligand. The identities of the small gold nanoclusters have been fully characterized by NMR, electrospray ionization mass spectrometry, elemental analysis, and single-crystal X-ray diffraction analysis. Octa- and undecagold clusters are found to display different UV−vis absorption behavior. The ligation of the bidentate ligands and halides or pseudohalides has resulted in the symmetry breaking of these nanoclusters with C_1 symmetry. The small gold nanoclusters with different coordinating halides or pseudohalides show distinct reactivities and stabilities in ligand/anion exchange experiments. The current research has provided insights into the origin of chirality in the diphosphine-stabilized small gold nanoclusters.

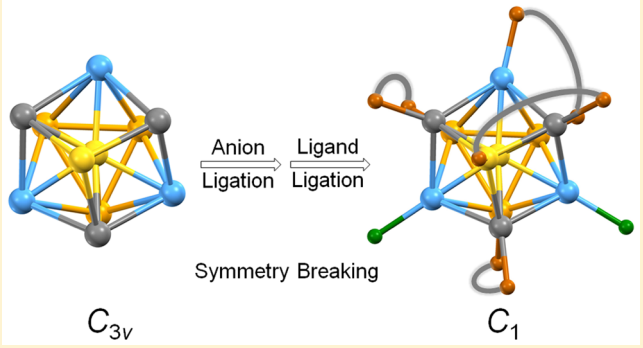

INTRODUCTION

In gold chemistry,[1] gold clusters are well known not only for their diverse configurations but also for their unique nuclearity and structure-dependent photophysical properties.[2] Sustained by gold−gold interactions,[3] numerous gold cluster assemblies have been reported in recent decades, including gold(I) clusters[4] and gold nanoclusters.[5] Gold nanoclusters with dimensions in the subnanometer size regime possess molecular characteristics, showing fascinating possibilities and opportunities in luminescence,[6a−c] nanomaterials,[2d] biology,[1c,2d,6d] sensing,[6e,f] catalysis,[6d,g−i] and so on. Given the unique structure-property relationship in the gold nanocluster systems, their nuclearity and symmetry would play important roles in determining their properties and potential applications.[1b,2d]

In recent years, great efforts have been made toward the synthesis and characterization of novel gold nanocluster structures with different nuclearities.[2g,5d,f,i,6c,7] In the synthetic chemistry of gold nanoclusters, difficulties have been encountered with precise control of size and shape as well as symmetry of the cluster structures.[1b] Recently, some research examples have been reported on the controlled formation of gold nanoclusters with given nuclearity and structures.[6d,e,8] These results revealed that the surface ligands and coordinating anions could be of relevance to the geometry and stability of the nanoclusters.

In the gold nanocluster system, thiols and phosphines are the most common coordinating ligands.[2h,5j,k,9a,b] Among the phosphine-coordinated gold nanoclusters, monodentate phosphines, especially triphenylphosphine and its derivatives, have been found to stabilize small gold nanoclusters with nuclearity from Au_4 to Au_{11}.[1a,2f,g,5a,j,9] Konishi and co-workers have reported several tetrahedron-based small gold cluster geometries stabilized by bidentate 1,3-bis(diphenylphosphino)-propane (dppp).[5c,e,g,6a,e] Bisphosphine (P^P)-stabilized small gold nanoclusters derived from a centered icosahedron have been much less reported.[6g,10] In 2003, Fujihara and co-workers reported the bidentate BINAP-stabilized nanospecies with chiroptical activity.[10a] Tsukuda and co-workers further confirmed them to be BINAP-stabilized undecagold clusters.[10b] These results together with subsequent theoretical studies achieved by Aikens and co-workers[10d] suggested that the ligation of bidentate phosphine ligands would affect the structures and chiroptical activity of the BINAP-stabilized undecagold clusters. However, the lack of single-crystal structures of this kind of diphosphine-stabilized small clusters has limited their studies and the identification of the nanoclusters.

It is anticipated that a knowledge of their X-ray crystal structures and their geometries would provide valuable information on their configurations and in-depth insights into the chirality origin of the undecagold clusters. In order to obtain an optimum P−P bite distance for the stabilization of the gold nanoclusters, diphosphines with appropriate bite distances have to be employed. Our strategy would be to use a diphosphine ligand that could have variable P−P bite distance

Received: September 28, 2016
Published: November 28, 2016

DOI: 10.1021/jacs.6b10168
J. Am. Chem. Soc. 2016, 138, 15736−15742

and flexibility. In this regard, the bidentate 1,1′-bis(diphenylphosphino)ferrocene (dppf), which is easily crystallized and has P−P distances comparable to those of BINAP and tunable P−P bite distances resulting from the rotation of the ferrocenyl moieties, was employed as the protecting ligand to construct small gold nanoclusters. Although dppf-gold(I) complexes have been rather frequently utilized as catalysts in organic synthetic chemistry,[11] their use in gold nanocluster systems is not that common.

Herein, a series of dppf-stabilized small gold nanoclusters has been successfully constructed and their single-crystal structures have been obtained, including octa- and undecagold nanoclusters. These newly constructed small gold super-atomic nanoclusters have been fully characterized by NMR, electrospray ionization mass spectrometry (ESI-MS), UV−vis absorption spectroscopy, elemental analysis, and single-crystal X-ray diffraction (XRD) analysis. The nuclearity-dependent photophysical behavior of the nanoclusters has been investigated. Both NMR spectroscopy and single-crystal XRD analysis have suggested the existence of symmetry breaking, which could be induced by ligation of the bidentate dppf ligand and halides/pseudohalides to the metal cores. Anion exchange properties of gold clusters with different counter-anions have been explored. The present work experimentally demonstrates the existence of ligation-induced symmetry breaking in the nanocluster system, providing important insights into the origin of chirality in small gold nanocluster systems.

RESULTS AND DISCUSSION

Synthesis and Characterization. By adding a freshly prepared ethanolic solution of $NaBH_4$ into a dichloromethane solution of $[(dppf)\{AuCl\}_2]$, a mixture of $[\mathbf{Au_{11}\text{-}Cl}]Cl$ and $[\mathbf{Au_8}]Cl_2$ has been obtained (Scheme 1). Vapor diffusion of diethyl ether into a dichloromethane solution of the residue gave complex $[\mathbf{Au_{11}\text{-}Cl}]Cl$ as a red solid. ^1H and $^{31}P\{^1H\}$ NMR spectra of $[\mathbf{Au_{11}\text{-}Cl}]Cl$ show complicated phosphorus and proton chemical environments with multiplet signals, indicating the unsymmetric structure of complex $[\mathbf{Au_{11}\text{-}Cl}]Cl$. In the positive-ion ESI-TOF mass spectrum of $[\mathbf{Au_{11}\text{-}Cl}]Cl$ (Figure 1a), the molecular ion peak observed at m/z 4454.55 and the close agreement of the simulated isotopic pattern have attributed the signal to the molecular ion cluster of $[(dppf)_4Au_{11}Cl_2]^+$ ($[\mathbf{Au_{11}\text{-}Cl}]^+$).

$[\mathbf{Au_8}]Cl_2$ was also obtained by recrystallization as dark-red crystals. $^{31}P\{^1H\}$ NMR and ^1H NMR analysis of the dark red crystals also indicated very complicated phosphorus and proton environments. The molecular ion clusters of $[\mathbf{Au_8}]Cl_2$, observed at m/z 3827.84 (M^+) and 1896.44 (M^{2+}) in the positive-ion ESI-TOF mass spectrum (Figure 1b), could be attributed to the molecular ions of this small gold nanocluster as $\{[(dppf)_4Au_8]Cl\}^+$ and $[(dppf)_4Au_8]^{2+}$. It was found that the reduction reaction of $[(dppf)\{AuCl\}_2]$ in ethanol with an excess of $NaBH_4$ would give a dark red solution, leading to the formation of octagold nanocluster $[\mathbf{Au_8}]Cl_2$ as the principal product (Scheme 1).

Other undecagold clusters, including $[(dppf)_4Au_{11}Br_2]Br$ ($[\mathbf{Au_{11}\text{-}Br}]Br$), $[(dppf)_4Au_{11}I_2]I$ ($[\mathbf{Au_{11}\text{-}I}]I$), and $[(dppf)_4Au_{11}(SCN)_2](SCN)$ ($[\mathbf{Au_{11}\text{-}SCN}]SCN$), were obtained using reaction procedures similar to that used for the cluster $[\mathbf{Au_{11}\text{-}Cl}]Cl$ but with dinuclear precursors $[(dppf)\{AuBr\}_2]$, $[(dppf)\{AuI\}_2]$, and $[(dppf)\{Au(SCN)\}_2]$, respectively. All the small gold nanoclusters were fully characterized by ^1H and $^{31}P\{^1H\}$ NMR, ESI-TOF-MS, UV−vis absorption spectroscopy, elemental analysis, and single-crystal XRD analysis.

Crystal Structure Determination. The solid-state structures of these small nanoclusters have further been confirmed by single-crystal XRD analysis. By slow vapor diffusion of diethyl ether into the acetonitrile solution of $[\mathbf{Au_{11}\text{-}Cl}]PF_6$, the dichloromethane−chloroform solution of $[\mathbf{Au_8}]Cl_2$, and dichloromethane−methanol solutions of $[\mathbf{Au_{11}\text{-}Br}]Br$, $[\mathbf{Au_{11}\text{-}I}]I$, and $[\mathbf{Au_{11}\text{-}SCN}]SCN$, crystals of the respective small gold nanoclusters suitable for X-ray structural determination were obtained. The undecagold complex $[\mathbf{Au_{11}\text{-}Cl}]PF_6$ is found to crystallize as red crystals in the triclinic space group $P\bar{1}$. As shown in Figure 2a, the structure consists of four dppf ligands and two chloro ligands ligated to an undecagold polyhedron that is derived from a centered icosahedron. The presence of two bound chlorides (Cl1 and Cl2) in the structure of the mono-positively charged cluster cation $\mathbf{Au_{11}\text{-}Cl}$ indicates the 8-electron superatom nature of this gold nanocluster. Octagold nanocluster $[\mathbf{Au_8}]Cl_2$ also crystallizes in the triclinic space group $P\bar{1}$. Four dppf ligands are ligated to all the eight gold atoms, indicating the absence of a centered gold atom and coordinating halides in the octagold cluster (Figure 2b). Seven gold atoms (Au2 to Au8) are found to form a pentagonal bipyramid, with another gold atom (Au1) attached to the exterior. The octagold core of $\mathbf{Au_8}$ could also be viewed as the undecagold core without the triangle formed by Au1, Au6, and Au7 of $\mathbf{Au_{11}\text{-}Cl}$. The octagold cluster with +2 charge is characteristic of a closed-shell structure with six electrons.

Similar to cluster cation $\mathbf{Au_{11}\text{-}Cl}$, other undecagold cluster cations $\mathbf{Au_{11}\text{-}Br}$, $\mathbf{Au_{11}\text{-}I}$, and $\mathbf{Au_{11}\text{-}SCN}$ also possess an undecagold polyhedron arrangement derived from a centered icosahedron. The bound phosphine and halo/pseudohalo ligands of these undecagold clusters are shown to be located at the same positions, in line with the related $[Au_{11}(PPh_3)_8Cl_2]Cl$ structure.[9b] The Au−Au bond distances of these small nanoclusters are in the range of 2.63−2.99 Å. All the Au−P bonds have lengths of around 2.3 Å in these small gold nanoclusters, while the lengths of the Au−X (X = Cl, Br, I, and SCN) bonds are different from each other. The lengths of the

Scheme 1. (a) Synthetic Routes for $[\mathbf{Au_{11}\text{-}Cl}]Cl$ and $[\mathbf{Au_8}]Cl_2$ from $[(dppf)\{AuCl\}_2]$ and (b) Chemical Structure Illustration of Undeca- and Octagold Nanoclusters

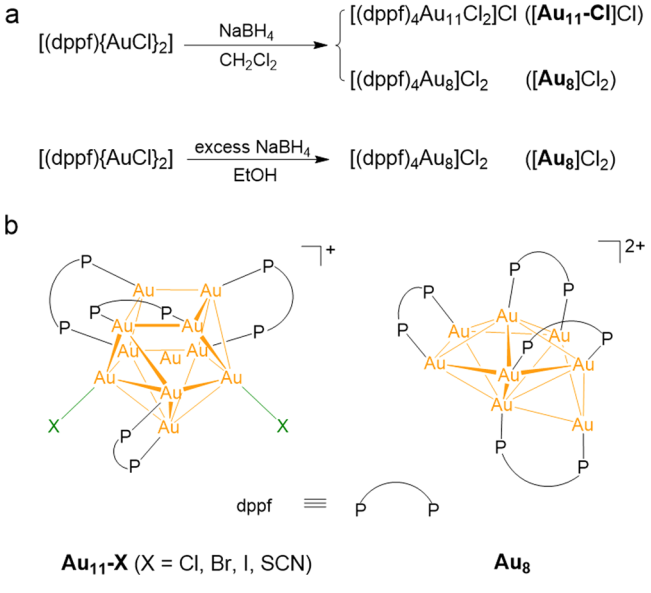

DOI: 10.1021/jacs.6b10168
J. Am. Chem. Soc. 2016, 138, 15736−15742

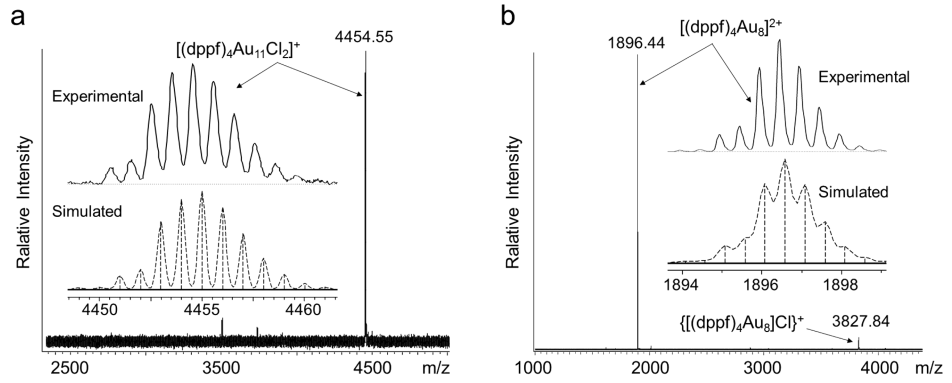

Figure 1. ESI mass spectra of (a) [**Au$_{11}$-Cl**]Cl and (b) [**Au$_8$**]Cl$_2$. The insets show the experimental and simulated isotope distribution of $[(dppf)_4Au_{11}Cl_2]^+$ ([**Au$_{11}$-Cl**]$^+$) and $[(dppf)_4Au_8]^{2+}$ ([**Au$_8$**]$^{2+}$).

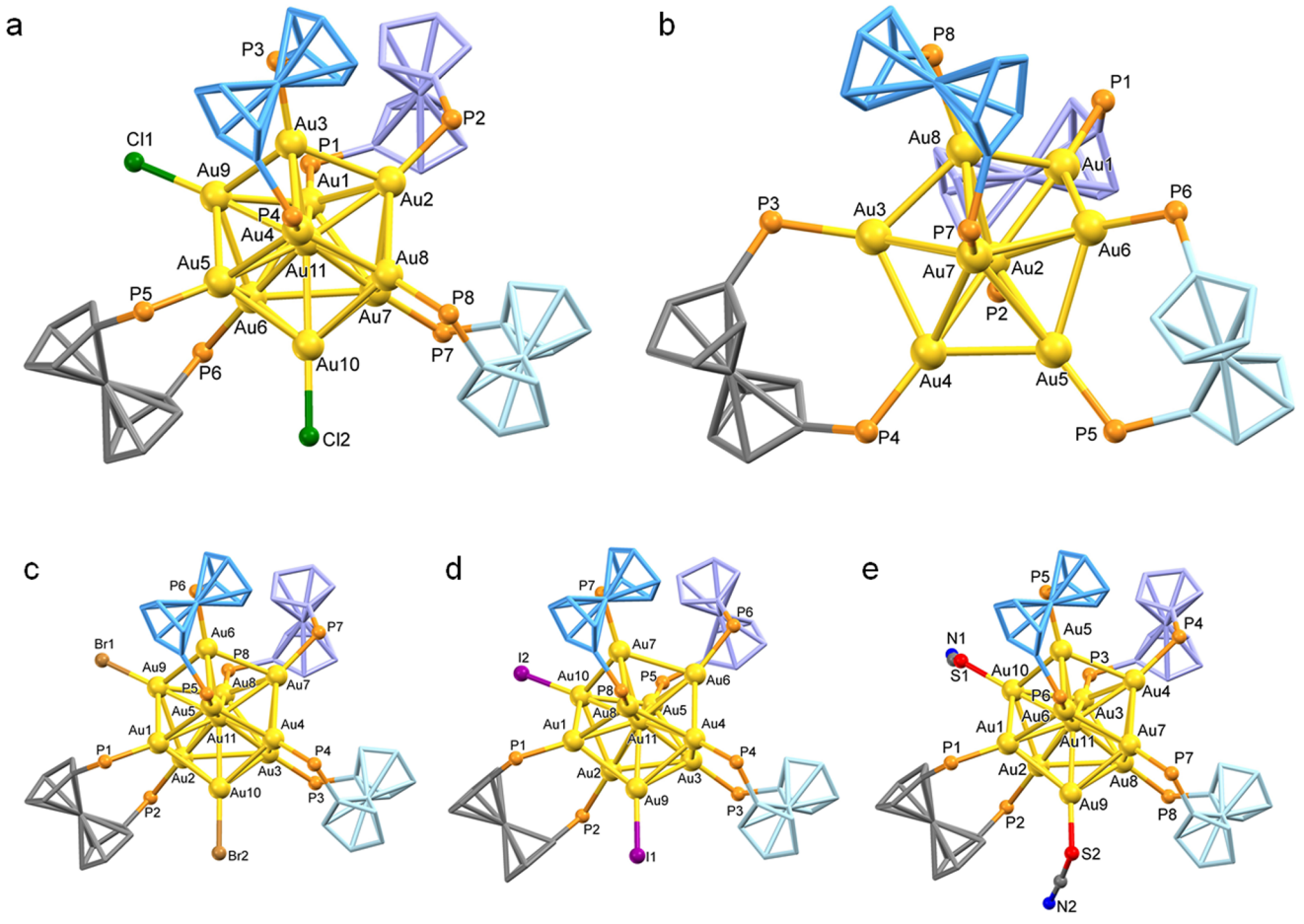

Figure 2. Crystal structures of small gold nanoclusters (a) [**Au$_{11}$-Cl**](PF$_6$), (b) [**Au$_8$**]Cl$_2$, (c) [**Au$_{11}$-Br**]Br, (d) [**Au$_{11}$-I**]I, and (e) [**Au$_{11}$-SCN**]SCN. The non-coordinated counter-anions, phenyl rings, and hydrogen atoms are omitted for clarity. Four ferrocene groups in each of these clusters are shown in four different colors.

Au−Cl bonds in cluster cation **Au$_{11}$-Cl** are about 2.37 Å, similar to those found in its analogues, $[Au_{11}(PPh_3)_7Cl_3]$ (2.37 Å) and $[Au_{11}(PPh_3)_8Cl_2]^+$ (2.36 Å).[5a,9b] The Au−Br, Au−I, and Au−S bond distances are found to be ca. 2.47, 2.62, and 2.35 Å, respectively. Bond lengths of Au−I in $[Au_{11}(PPh_3)_7I_3]$ have also been reported to be about 2.62 Å.[12a] The increase in Au−X bond lengths from Cl to Br and I is in line with the larger atomic radii for Br and I. The non-coordinating counter-anions as well as the solvent molecules were located in the crystal lattice and were found to be attached to the molecular cluster cations through hydrogen bonding, as revealed in the crystal packing diagram.

Structure-Dependent Photophysical Properties. As was demonstrated previously, the UV−vis absorptions of phosphorus ligand-stabilized gold nanoclusters are mainly determined by their metal core structures and are less influenced by the surface ligands. As shown in Figure 3a, nanoclusters with different nuclearity (undecanuclear [**Au$_{11}$-Cl**]Cl versus octanuclear [**Au$_8$**]Cl$_2$) have led to differences in their UV−vis spectra. In the UV−vis absorption spectrum of the

DOI: 10.1021/jacs.6b10168
J. Am. Chem. Soc. 2016, 138, 15736−15742

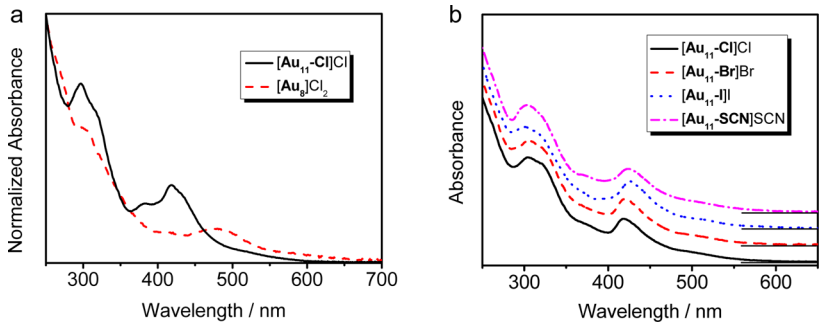

Figure 3. UV−vis absorption spectra showing differences in the peak positions of (a) small gold clusters with different nuclearity and (b) undecanuclear clusters with different coordinating anions in CH_2Cl_2. The baseline of the UV−vis spectra has been displaced for better display and ease of comparison.

octagold cluster [**Au$_8$**]Cl$_2$ in dichloromethane, two absorption maxima at 298 and 478 nm and a shoulder at 580 nm are observed, whereas the respective signals of undecagold [**Au$_{11}$-Cl**]Cl are located at 304, 418, and 515 nm. Obvious red shifts of the lower-energy absorption bands from 418 and 515 to 478 and 580 nm are in line with the distinct colors of [**Au$_{11}$-Cl**]Cl (orange red) and [**Au$_8$**]Cl$_2$ (dark red) in solution. The absorption bands for small gold nanoclusters have been attributed to transitions among the molecular orbitals of the polynuclear metal core. Different electronic configurations of 8-electron for **Au$_{11}$-Cl** and 6-electron for **Au$_8$** are believed to be responsible for the attractive structurally dependent photophysical properties.[12b]

The structures and symmetry of these undecagold nanoclusters ([**Au$_{11}$-Cl**]Cl, [**Au$_{11}$-Br**]Br, [**Au$_{11}$-I**]I, and [**Au$_{11}$-SCN**]SCN) are similar to each other. As a result, nearly the same electronic absorption spectral patterns are observed in their UV−vis absorption spectra. As shown in Figure 3b, two absorption maxima at around 300 and 420 nm are found in the UV−vis spectra of the undecagold clusters. However, a slight wavelength shift could be observed with a change in the coordinating anions. For instance, the lower-energy bands of [**Au$_{11}$-Cl**]Cl, [**Au$_{11}$-Br**]Br, and [**Au$_{11}$-I**]I are located at 418, 421, and 426 nm, respectively. Even though the shifts were found to be very slight, the order of the absorption energy of the lower-energy bands is **Au$_{11}$-Cl** > **Au$_{11}$-Br** > **Au$_{11}$-I**, which is in line with the electronegativity order of the relevant coordinating anions Cl^- > Br^- > I^-. This trend might suggest the existence of ligand-mediated transitions in the electronic absorptions of this type of nanocluster system, involving some ligand-to-metal charge transfer (LMCT) or ligand-to-metal−metal charge transfer (LMMCT) character.

Ligation-Driven Symmetry Breaking. Previous examples of triphenylphosphine-stabilized small gold nanoclusters mostly showed very symmetrical structures with only one signal in their $^{31}P\{^1H\}$ NMR spectra.[5a,9b,12b] However, rather complicated proton and phosphorus chemical environments are found in the NMR studies of the nanoclusters in the current work, indicating the highly unsymmetrical structures of these nanoclusters. For cluster [**Au$_{11}$-SCN**]SCN, as shown in Figure 4a, 23 singlets were observed in the region of ca. δ 2.6−5.7 ppm in the ^1H NMR spectrum, corresponding to the 32 protons of the ferrocenyl moieties in one cluster molecule, while the signals from ca. δ 6.1 to 8.2 ppm are attributed to protons of the phenyl rings. Meanwhile, the $^{31}P\{^1H\}$ NMR spectrum of [**Au$_{11}$-SCN**]SCN exhibits eight sets of signals at δ 42.8, 44.9, 46.8, 48.0, 49.4, 50.3, 51.0, and 55.1 ppm with equal integral

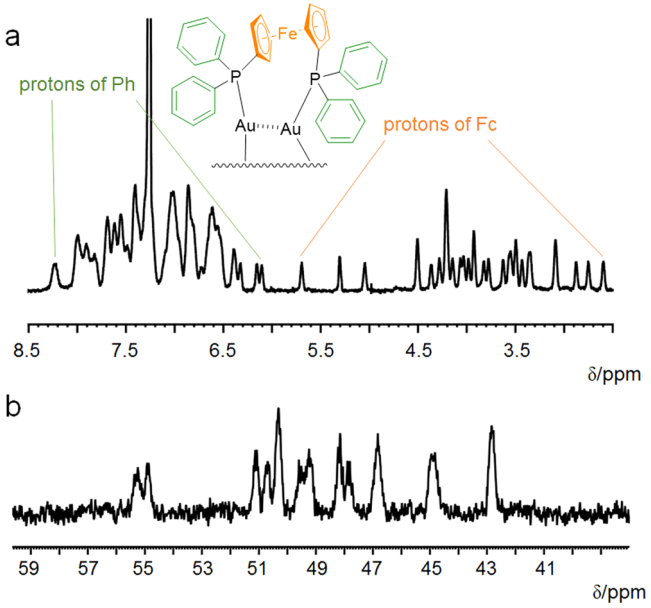

Figure 4. (a) ^1H and (b) $^{31}P\{^1H\}$ NMR spectra of undecagold nanocluster [**Au$_{11}$-SCN**]SCN in $CDCl_3$.

ratios (Figure 4b), indicating eight different phosphorus chemical environments. In fact, there are only eight P atoms in one cluster molecule, which indicates that none of the eight phosphorus atoms in one cluster molecule could be interchanged by any symmetry operations, even in the solution state.

Similarly, eight phosphorus environments are observed for [**Au$_{11}$-Br**]Br and [**Au$_{11}$-I**]I. Although only six different phosphorus chemical environments are observed for [**Au$_{11}$-Cl**]Cl, these results still demonstrate the highly unsymmetrical structures of these Au_{11} clusters with C_1 symmetry point group, which has been further revealed by their X-ray single-crystal analysis. However, all the small gold nanoclusters crystallize in the centrosymmetric space groups, triclinic $P\bar{1}$ and monoclinic $C2/c$, indicating the racemic nature of these small gold clusters. Nevertheless, if only the undecagold cluster cores are considered, the symmetry could be approximated to a C_{3v} point group (Figure 5), which has also been observed in studies on related Au_{11} nanoclusters, $[Au_{11}(PPh_3)_8Cl_2]^+$ and $[Au_{11}(PPh_3)_7Cl_3]$.[5a,9b] After coordination of two chloro groups, the symmetry could be lowered from approximate C_{3v} to C_s (Figure 5). Finally, the ligation of bidentate dppf would break all the symmetry, giving the highly unsymmetrical Au_{11} cluster

DOI: 10.1021/jacs.6b10168
J. Am. Chem. Soc. 2016, 138, 15736−15742

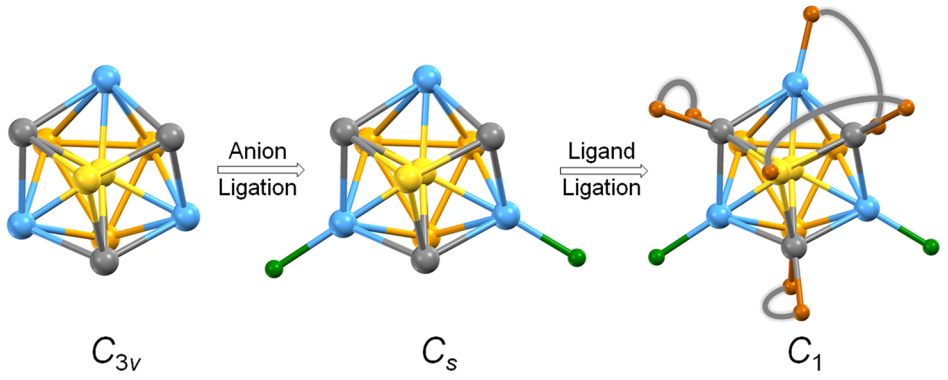

Figure 5. Illustration of ligation-driven symmetry breaking from C_{3v} point group of the undecagold core to C_1 point group of the cluster cation. A C_3 axis and three σ_v planes of the undecagold core (left) are along the two gold atoms in yellow and the other three colors (grey, blue, and orange) represent the three different Au environments. Green balls in the middle and right panel are representative of halides/pseudohalides, and dppf ligands in the right panel are illustrated by two brown balls linked by a grey belt.

molecules of C_1 symmetry group. For the octagold nanocluster [**Au$_8$**]Cl$_2$, the symmetry of the naked octagold core is distorted C_s. The arrangement of four dppf ligands on the surface has led to the reduction of symmetry from C_s to C_1. The ligation of the diphosphine ligands and halides/pseudohalides has resulted in the symmetry decrease of the polynuclear gold cores, giving rise to the unsymmetrical small gold nanoclusters.

Ligand and Anion Exchange Experiments. The monophosphine-protected small gold nanoclusters have been found to undergo further aggregation through ligand exchange.[9b,12c,d] By ligand exchange with glutathione (GSH), triphenylphosphine-stabilized undecagold nanoclusters, [Au$_{11}$(PPh$_3$)$_7$Cl$_3$] and [Au$_{11}$(PPh$_3$)$_8$Cl$_2$]Cl, are reported to yield Au$_{25}$ or other small clusters.[9b,12d] Nevertheless, the ligand exchange has never been applied to diphosphine-stabilized small gold nanoclusters. Herein, the stability and ligand exchange properties of the octa- or undecagold clusters are also explored. An excess of GSH was reacted with these diphosphine-stabilized small nanoclusters in a biphasic (CHCl$_3$−H$_2$O) system. However, the aqueous phase remained colorless even after the reaction temperature reached 55 °C, suggesting the absence of ligand exchange reactions. This phenomenon revealed that, compared to the monodentate PPh$_3$ ligands, the bidentate dppf ligands have dramatically enhanced the stability of the small gold nanoclusters.

Since the dinuclear precursors, [(dppf){AuBr}$_2$], [(dppf){AuI}$_2$], and [(dppf){Au(SCN)}$_2$], are obtained by exchanging the corresponding halides/pseudohalides with [(dppf){AuCl}$_2$], anion exchange experiments of the small gold nanoclusters have also been carried out. Undecagold cluster [**Au$_{11}$-Cl**]Cl was used to react with respective KBr, KI, and KSCN. From the experiments, it could be found that [**Au$_{11}$-Cl**]Cl could undergo exchange with all of these anions to give clusters [**Au$_{11}$-Br**]Br, [**Au$_{11}$-I**]I, and [**Au$_{11}$-SCN**]SCN. On the other hand, [**Au$_{11}$-I**]I appears to be the most stable cluster, which could be obtained from cluster cations **Au$_{11}$-Cl**, **Au$_{11}$-Br**, and **Au$_{11}$-SCN** via their exchange with I$^-$. The stability order of these undecagold nanoclusters is assigned as **Au$_{11}$-I** > **Au$_{11}$-SCN** > **Au$_{11}$-Br** > **Au$_{11}$-Cl**.

The anion exchange reactions of [**Au$_{11}$-Cl**]Cl and [**Au$_{11}$-Br**]Br with KI are found to be very fast and would be completed within 30 min, whereas anion exchange from SCN$^-$ to I$^-$ is much slower. As revealed by the ^{31}P{^{1}H} NMR monitoring experiments (Figure 6), after 30 min, the majority of [**Au$_{11}$-SCN**]SCN would remain unchanged. After 24 h, although most of [**Au$_{11}$-SCN**]SCN has been converted to [**Au$_{11}$-I**]I, signals of

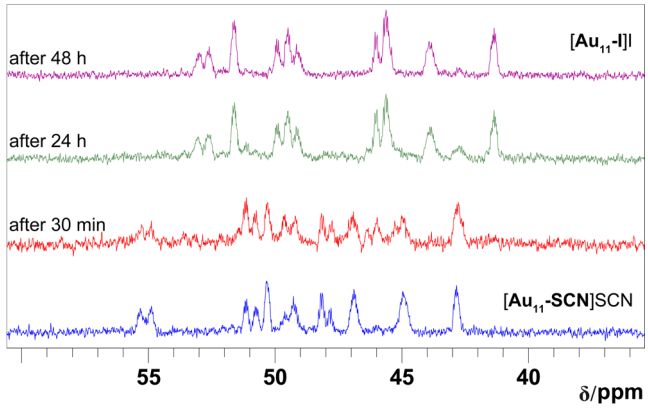

Figure 6. ^{31}P{^{1}H} NMR spectral changes of cluster [**Au$_{11}$-SCN**]SCN upon reaction with an excess of KI in biphasic CDCl$_3$−H$_2$O.

[**Au$_{11}$-SCN**]SCN could still be observed in the NMR spectra. Finally, NMR studies indicate that the anion exchange from SCN$^-$ to I$^-$ would be completed only after more than 48 h.

Octagold nanocluster [**Au$_8$**]Cl$_2$ has also been subjected to the biphasic solution system in the presence of KX (X = Cl, Br, I, and SCN). No reaction occurs for KCl and KBr, but cluster transformation from the octagold cluster to the undecagold clusters is observed for KSCN and KI (Figure 7). These results suggest that the reactivity and stability of the small gold nanoclusters could be affected by the protecting ligands, the nuclearity, and the coordinating anions.

■ CONCLUSION

A series of dppf-stabilized octa- and undecagold nanoclusters have been developed. Unlike the monophosphine-stabilized gold nanoclusters, which have been found to undergo ligand exchange reactions to give thiol-stabilized gold nanoclusters, the use of dppf ligands has been found to confer higher stability to the small gold nanoclusters, preventing them from undergoing ligand exchange even in the presence of an excess of thiol ligands. On the other hand, the undecagold nanoclusters with different coordinated halides or pseudohalides could be interconverted through anion exchange reactions, whereas the octagold nanoclusters without coordinated halides/pseudohalides are found to undergo further aggregation to give undecagold nanoclusters only in the presence of an excess of KSCN and KI, but with no reaction with KCl and KBr. These

DOI: 10.1021/jacs.6b10168
J. Am. Chem. Soc. 2016, 138, 15736−15742

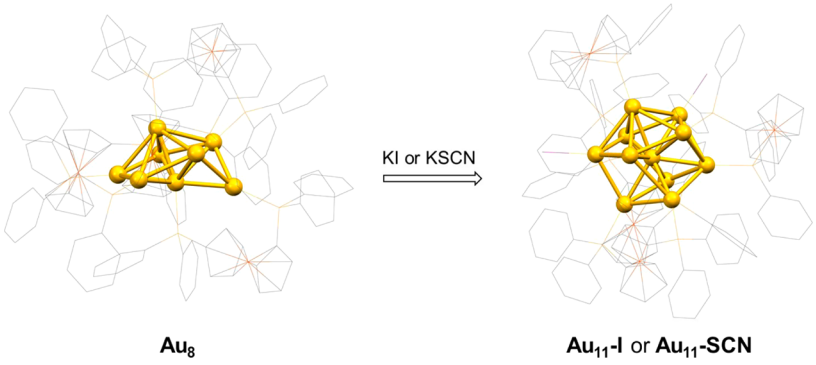

Figure 7. Cluster core changes in the presence of an excess of KI or KSCN in biphasic solvents.

results demonstrate that the protecting ligands as well as the coordinated halides/pseudohalides play significant roles in governing the stabilities and reactivities of small gold nanoclusters, which would provide important insights into their structure-property relationships and guiding principles for the future design and synthesis of novel gold nanoclusters. In addition, NMR and X-ray diffraction studies of the nanoclusters also reveal their unsymmetrical structure with C_1 symmetry, which has never been observed in monophosphine-stabilized small gold nanoclusters. The symmetry breaking has been caused by ligation of anions and ligands to the Au surface atoms of the gold clusters. The current work should be beneficial in that it reveals the origin of chirality in the nanoclusters.

■ ASSOCIATED CONTENT

Supporting Information

The Supporting Information is available free of charge on the ACS Publications website at DOI: 10.1021/jacs.6b10168.

Synthesis and characterization and X-ray structure determination (PDF)
Crystallographic details for [Au_{11}-Cl] (CIF)
Crystallographic details for [Au_8] (CIF)
Crystallographic details for [Au_{11}-Br] (CIF)
Crystallographic details for [Au_{11}-I] (CIF)
Crystallographic details for [Au_{11}-SCN] (CIF)

■ AUTHOR INFORMATION

Corresponding Author

*wwyam@hku.hk

Notes

The authors declare no competing financial interest.

■ ACKNOWLEDGMENTS

This work was supported by the University Grants Committee Areas of Excellence Scheme (AoE/P-03/08), the ANR/RGC Joint Research Scheme (A-HKU704/12), and a General Research Fund (GRF) Grant from the Research Grants Council of the Hong Kong Special Administrative Region, P. R. China (HKU 17304715). V.W.-W.Y. acknowledges support from The University of Hong Kong under the Strategic Research Theme on New Materials. L.-Y.Y. acknowledges the receipt of a postgraduate studentship from The University of Hong Kong. The Beijing Synchrotron Radiation Facility (BSRF) is also thanked for providing beamline time of the synchrotron radiation facilities. Dr. Lap Szeto is acknowledged for her assistance in X-ray crystal data collection. The authors would like to thank Mr. Hao Li and Prof. Shu-Yan Yu for their assistance in mass spectrometry measurements.

■ REFERENCES

(1) (a) Schmidbaur, H., Ed. *Gold: Progress in Chemistry, Biochemistry and Technology*; John Wiley & Sons Ltd: Chichester, England, 1999. (b) Laguna, A., Ed. *Modern Supramolecular Gold Chemistry: Gold-Metal Interactions and Applications*; Wiley: Weinheim, Germany, 2008. (c) Mohr, F., Ed. *Gold Chemistry: Applications and Future Directions in the Life Sciences*; Wiley-VCH Verla GmbH & Co. KGaA: Weinheim, Germany, 2009.

(2) (a) Che, C.-M.; Lai, S.-W. *Coord. Chem. Rev.* **2005**, *249*, 1296. (b) Gimeno, M. C.; Laguna, A. *Chem. Soc. Rev.* **2008**, *37*, 1952. (c) Puddephatt, R. J. *Chem. Soc. Rev.* **2008**, *37*, 2012. (d) Yang, X.; Yang, M.-X.; Pang, B.; Vara, M.; Xia, Y.-N. *Chem. Rev.* **2015**, *115*, 10410. (e) Yam, V. W.-W.; Au, V. K.-M.; Leung, S. Y.-L. *Chem. Rev.* **2015**, *115*, 7589. (f) Mingos, D. M. P. *Dalton Trans.* **2015**, *44*, 6680. (g) Fang, J.; Zhang, B.; Yao, Q.; Yang, Y.; Xie, J.; Yan, N. *Coord. Chem. Rev.* **2016**, *322*, 1. (h) Häkkinen, H. *Nat. Chem.* **2012**, *4*, 443.

(3) (a) Scherbaum, F.; Grohmann, A.; Huber, B.; Kruger, C.; Schmidbaur, H. *Angew. Chem., Int. Ed. Engl.* **1988**, *27*, 1544. (b) Pyykkö, P. *Chem. Rev.* **1997**, *97*, 597. (c) Schmidbaur, H.; Schier, A. *Chem. Soc. Rev.* **2012**, *41*, 370.

(4) (a) Chen, J. H.; Mohamed, A. A.; Abdou, H. E.; Bauer, J. A. K.; Fackler, J. P., Jr.; Bruce, A. E.; Bruce, M. R. M. *Chem. Commun.* **2005**, 1575. (b) Gussenhoven, E. M.; Fettinger, J. C.; Pham, D. M.; Malwitz, M. M.; Balch, A. L. *J. Am. Chem. Soc.* **2005**, *127*, 10838. (c) Chui, S. S.-Y.; Chen, R.; Che, C.-M. *Angew. Chem., Int. Ed.* **2006**, *45*, 1621. (d) Sevillano, P.; Fuhr, O.; Kattannek, M.; Nava, P.; Hampe, O.; Lebedkin, S.; Ahlrichs, R.; Fenske, D.; Kappes, M. M. *Angew. Chem., Int. Ed.* **2006**, *45*, 3702. (e) Lee, T. K.-M.; Zhu, N.-Y.; Yam, V. W.-W. *J. Am. Chem. Soc.* **2010**, *132*, 17646. (f) Koshevoy, I. O.; Lin, C. L.; Karttunen, A. J.; Haukka, M.; Shih, C. W.; Chou, P. T.; Tunik, S. P.; Pakkanen, T. A. *Chem. Commun.* **2011**, *47*, 5533. (g) Ni, W. X.; Li, M.; Zheng, J.; Zhan, S. Z.; Qiu, Y. M.; Ng, S. W.; Li, D. *Angew. Chem., Int. Ed.* **2013**, *52*, 13472. (h) Hau, F. K.-W.; Lee, T. K.-M.; Cheng, E. C.-C.; Au, V. K.-M.; Yam, V. W.-W. *Proc. Natl. Acad. Sci. U. S. A.* **2014**, *111*, 15900. (i) Lee, T. K.-M.; Cheng, E. C.-C.; Zhu, N.-Y.; Yam, V. W.-W. *Chem. - Eur. J.* **2014**, *20*, 304. (j) Yao, L.-Y.; Hau, F. K.-W.; Yam, V. W.-W. *J. Am. Chem. Soc.* **2014**, *136*, 10801. (k) Yao, L.-Y.; Yam, V. W.-W. *J. Am. Chem. Soc.* **2015**, *137*, 3506. (l) Yao, L.-Y.; Lee, T. K.-M.; Yam, V. W.-W. *J. Am. Chem. Soc.* **2016**, *138*, 7260.

(5) (a) Gutrath, B. S.; Englert, U.; Wang, Y. T.; Simon, U. *Eur. J. Inorg. Chem.* **2013**, *2013*, 2002. (b) Gutrath, B. S.; Oppel, I. M.; Presly, O.; Beljakov, I.; Meded, V.; Wenzel, W.; Simon, U. *Angew. Chem., Int. Ed.* **2013**, *52*, 3529. (c) Kobayashi, N.; Kamei, Y.; Shichibu, Y.; Konishi, K. *J. Am. Chem. Soc.* **2013**, *135*, 16078. (d) Chen, J.; Zhang, Q. F.; Bonaccorso, T. A.; Williard, P. G.; Wang, L. S. *J. Am. Chem. Soc.* **2014**, *136*, 92. (e) Shichibu, Y.; Zhang, M. Z.; Kamei, Y.; Konishi, K. *J. Am. Chem. Soc.* **2014**, *136*, 12892. (f) Wan, X. K.; Yuan, S. F.; Lin, Z. W.; Wang, Q. M. *Angew. Chem., Int. Ed.* **2014**, *53*, 2923. (g) Sugiuchi, M.; Shichibu, Y.; Nakanishi, T.; Hasegawa, Y.; Konishi, K. *Chem.*

DOI: 10.1021/jacs.6b10168
J. Am. Chem. Soc. 2016, 138, 15736−15742

Commun. **2015**, *51*, 13519. (h) Wan, X. K.; Xu, W. W.; Yuan, S. F.; Gao, Y.; Zeng, X. C.; Wang, Q. M. *Angew. Chem., Int. Ed.* **2015**, *54*, 9683. (i) Wang, Y.; Su, H. F.; Xu, C. F.; Li, G.; Gell, L.; Lin, S. C.; Tang, Z. C.; Häkkinen, H.; Zheng, N. F. *J. Am. Chem. Soc.* **2015**, *137*, 4324. (j) Yao, H.; Iwatsu, M. *Langmuir* **2016**, *32*, 3284. (k) Knoppe, S.; Bürgi, T. *Acc. Chem. Res.* **2014**, *47*, 1318.

(6) (a) Shichibu, Y.; Kamei, Y.; Konishi, K. *Chem. Commun.* **2012**, *48*, 7559. (b) Kang, X.; Wang, S. X.; Song, Y. B.; Jin, S.; Sun, G. D.; Yu, H. Z.; Zhu, M. Z. *Angew. Chem., Int. Ed.* **2016**, *55*, 3611. (c) Yu, Y.; Luo, Z. T.; Chevrier, D. M.; Leong, D. T.; Zhang, P.; Jiang, D. E.; Xie, J. P. *J. Am. Chem. Soc.* **2014**, *136*, 1246. (d) de Silva, N.; Ha, J. M.; Solovyov, A.; Nigra, M. M.; Ogino, I.; Yeh, S. W.; Durkin, K. A.; Katz, A. *Nat. Chem.* **2010**, *2*, 1062. (e) Kamei, Y.; Shichibu, Y.; Konishi, K. *Angew. Chem., Int. Ed.* **2011**, *50*, 7442. (f) Paau, M. C.; Lo, C. K.; Yang, X. P.; Choi, M. M. F. *J. Phys. Chem. C* **2010**, *114*, 15995. (g) Andreiadis, E. S.; Vitale, M. R.; Mezailles, N.; Le Goff, X.; Le Floch, P.; Toullec, P. Y.; Michelet, V. *Dalton Trans.* **2010**, *39*, 10608. (h) Liu, J.; Krishna, K. S.; Losovyj, Y. B.; Chattopadhyay, S.; Lozova, N.; Miller, J. T.; Spivey, J. J.; Kumar, C. S. S. R. *Chem. - Eur. J.* **2013**, *19*, 10201. (i) Wang, Y.; Wan, X. K.; Ren, L. T.; Su, H. F.; Li, G.; Malola, S.; Lin, S. C.; Tang, Z. C.; Häkkinen, H.; Teo, B. K.; Wang, Q. M.; Zheng, N. F. *J. Am. Chem. Soc.* **2016**, *138*, 3278.

(7) (a) Chen, Y. X.; Zeng, C. J.; Liu, C.; Kirschbaum, K.; Gayathri, C.; Gil, R. R.; Rosi, N. L.; Jin, R. C. *J. Am. Chem. Soc.* **2015**, *137*, 10076. (b) Lechtken, A.; Schooss, D.; Stairs, J. R.; Blom, M. N.; Furche, F.; Morgner, N.; Kostko, O.; von Issendorff, B.; Kappes, M. M. *Angew. Chem., Int. Ed.* **2007**, *46*, 2944. (c) Walter, M.; Moseler, M.; Whetten, R. L.; Häkkinen, H. *Chem. Sci.* **2011**, *2*, 1583. (d) Malola, S.; Lehtovaara, L.; Knoppe, S.; Hu, K. J.; Palmer, R. E.; Bürgi, T.; Häkkinen, H. *J. Am. Chem. Soc.* **2012**, *134*, 19560. (e) AbdulHalim, L. G.; Bootharaju, M. S.; Tang, Q.; Del Gobbo, S.; AbdulHalim, R. G.; Eddaoudi, M.; Jiang, D. E.; Bakr, O. M. *J. Am. Chem. Soc.* **2015**, *137*, 11970.

(8) (a) Bertino, M. F.; Sun, Z. M.; Zhang, R.; Wang, L. S. *J. Phys. Chem. B* **2006**, *110*, 21416. (b) Pettibone, J. M.; Hudgens, J. W. *J. Phys. Chem. Lett.* **2010**, *1*, 2536. (c) Luo, Z. T.; Nachammai, V.; Zhang, B.; Yan, N.; Leong, D. T.; Jiang, D. E.; Xie, J. P. *J. Am. Chem. Soc.* **2014**, *136*, 10577. (d) Knoppe, S.; Azoulay, R.; Dass, A.; Bürgi, T. *J. Am. Chem. Soc.* **2012**, *134*, 20302.

(9) (a) Jin, R. C. *Nanoscale* **2010**, *2*, 343. (b) McKenzie, L. C.; Zaikova, T. O.; Hutchison, J. E. *J. Am. Chem. Soc.* **2014**, *136*, 13426. (c) Bartlett, P. A.; Bauer, B.; Singer, S. J. *J. Am. Chem. Soc.* **1978**, *100*, 5085. (d) Manassero, M.; Naldini, L.; Sansoni, M. *J. Chem. Soc., Chem. Commun.* **1979**, 385. (e) Jaw, H. R. C.; Mason, W. R. *Inorg. Chem.* **1991**, *30*, 3552. (f) Laguna, A.; Laguna, M.; Gimeno, M. C.; Jones, P. G. *Organometallics* **1992**, *11*, 2759.

(10) (a) Tamura, M.; Fujihara, H. *J. Am. Chem. Soc.* **2003**, *125*, 15742. (b) Yanagimoto, Y.; Negishi, Y.; Fujihara, H.; Tsukuda, T. *J. Phys. Chem. B* **2006**, *110*, 11611. (c) Smits, J. M. M.; Bour, J. J.; Vollenbroek, F. A.; Beurskens, P. T. *J. Crystallogr. Spectrosc. Res.* **1983**, *13*, 355. (d) Provorse, M. R.; Aikens, C. M. *J. Am. Chem. Soc.* **2010**, *132*, 1302.

(11) Driver, M. S.; Hartwig, J. F. *J. Am. Chem. Soc.* **1996**, *118*, 7217.

(12) (a) Vollenbroek, F. A.; Bouten, P. C. P.; Trooster, J. M.; Vandenberg, J. P.; Bour, J. *Inorg. Chem.* **1978**, *17*, 1345. (b) Gutrath, B. S.; Schiefer, F.; Homberger, M.; Englert, U.; Serb, M. D.; Bettray, W.; Beljakov, I.; Meded, V.; Wenzel, W.; Simon, U. *Eur. J. Inorg. Chem.* **2016**, *2016*, 975. (c) Woehrle, G. H.; Warner, M. G.; Hutchison, J. E. *J. Phys. Chem. B* **2002**, *106*, 9979. (d) Shichibu, Y.; Negishi, Y.; Tsukuda, T.; Teranishi, T. *J. Am. Chem. Soc.* **2005**, *127*, 13464.

DOI: 10.1021/jacs.6b10168
J. Am. Chem. Soc. 2016, 138, 15736−15742